

# Relative effects of wind stress curl, topography, and stratification on large-scale circulation in Lake Michigan

David J. Schwab

NOAA Great Lakes Environmental Research Laboratory, Ann Arbor, Michigan, USA

Dmitry Beletsky

Department of Naval Architecture and Marine Engineering, University of Michigan, Ann Arbor, Michigan, USA

Received 25 July 2001; revised 9 January 2002; accepted 19 April 2002; published 21 February 2003.

[1] This paper uses the results from two multiseason numerical model simulations of Lake Michigan hydrodynamics to examine the relative effects of wind stress curl, topography, and stratification on large-scale circulation. The multiseason simulations provide a period long enough to encompass the full range of atmospheric and thermal conditions that can occur in the lake. The purpose of this paper is to diagnose the relative importance of various mechanisms responsible for the large-scale circulation patterns by analyzing the vorticity balance in the lake on a monthly timescale. Five different model scenarios are used to isolate the predominant mechanisms: (1) baroclinic lake, spatially variable wind stress; (2) barotropic lake, spatially variable wind stress; (3) baroclinic lake, spatially uniform wind stress; (4) barotropic lake, spatially uniform wind stress; and (5) barotropic lake, linearized equations, spatially uniform wind stress. By comparing the results of these five model scenarios it is shown that the cyclonic wind stress curl in the winter and the effect of baroclinicity in the summer are primarily responsible for the predominantly cyclonic flow in the lake. Topographic effects are also important but are not as significant as wind stress curl and baroclinic effects. Nonlinear effects are much smaller. **INDEX TERMS:** 4239 Oceanography: General: Limnology; 4243 Oceanography: General: Marginal and semiencllosed seas; 4255 Oceanography: General: Numerical modeling; 4512 Oceanography: Physical: Currents; **KEYWORDS:** wind stress curl, vorticity, lake circulation

**Citation:** Schwab, D. J., and D. Beletsky, Relative effects of wind stress curl, topography, and stratification on large-scale circulation in Lake Michigan, *J. Geophys. Res.*, 108(C2), 3044, doi:10.1029/2001JC001066, 2003.

## 1. Introduction

[2] Since the pioneering numerical modeling studies of Rao and Murty [1970] and Murty and Rao [1970] on the steady state, wind-induced circulation in the Great Lakes, there continues to be uncertainty about the relative effects of wind stress curl, topography, and stratification on large-scale circulation in the Great Lakes and other water bodies. The Rao and Murty studies showed that the large-scale steady state circulation pattern due to a uniform wind stress generally consists of a pair of counter-rotating gyres with downwind flow near the shores and upwind return flow in the deeper parts of the basin. The pattern is strongly controlled by bottom topography. They also showed that wind stress curl tended to enhance the circulatory gyre that had the same sense of rotation as the wind curl. These results were consistent with analytical studies of steady state circulation by Birchfield [1967], but there were no direct observations of large-scale circulations with which to adequately test these results until the

International Field Year on the Great Lakes (IFYGL) in Lake Ontario in 1972.

[3] In one of the first results of IFYGL, Pickett and Richards [1975] described the circulation observed from an extensive array of current meter moorings in Lake Ontario during July 1972 as “two counterclockwise gyres side-by-side in apparent geostrophic balance”, which contradicted the steady, wind-induced solution. Apparently stratification was more important than wind forcing during this period. Later, the IFYGL currents in November 1972 were analyzed by Pickett [1976] to reveal a single cyclonic gyre, which seemed to indicate the dominance of wind stress curl during this period. He did however note that gaps in the current meter network could have prevented the observation of the anticyclonic gyre where the steady state model would have predicted it to exist for the prevailing wind direction. The final analysis of all the IFYGL current meter data for the nonstratified period by Pickett [1977] showed several months with the expected two-gyre steady state circulation pattern, but several other months with only a single cyclonic gyre. Pickett [1977] also concluded that during the months when a single gyre circulation pattern was observed, the wind field vorticity did not appear to be

strong enough to overwhelm the two-gyre, wind-induced circulation pattern.

[4] *Csanady* [1978] developed a theory for mean circulation in the coastal zone based on a succession of wind-induced topographic waves, which can establish a mean coastal current counter to the wind, the so-called “arrested topographic wave”. This theory was invoked as a possible explanation of *Pickett’s* [1977] observations of Lake Ontario’s mean winter circulation.

[5] *Schwab* [1983] examined the dynamics of steady state and low frequency ( $<0.6$  cpd) oscillating currents in Lake Michigan. Time series of currents from his numerical model results compared well with the observed current meter time series from a transect of moorings across the lake and an along-shore array on the east coast. The calculated two-gyre steady state circulation pattern did not agree with observed mean currents from May–November 1976, which indicated predominantly cyclonic circulation.

[6] The low frequency oscillations in southern Lake Michigan during the 1976 field program were interpreted as the lowest mode topographic wave in the southern basin by *Saylor et al.* [1980]. The topographic wave consists of two counter-rotating gyres which propagate cyclonically around the basin with a period of about 4 days. The mean currents during three 2-month periods in 1976 showed evidence of a weak two gyre steady circulation in the spring and summer, but a single cyclonic gyre in the fall.

[7] An analysis of Lake Michigan current meter data from 1982–1983 by *Beletsky et al.* [1999] revealed predominantly cyclonic circulation in both the northern and southern basins in summer and winter, with winter circulation dominating the annual average. They also examined long-term current measurements from the other four Great Lakes. They found that the circulation patterns showed a tendency to be cyclonic in the larger lakes (Superior, Michigan, and Huron), especially in winter. The smaller lakes (Ontario and Erie) were more likely to exhibit a two-gyre circulation pattern. They speculated that lake-induced mesoscale vorticity in the atmosphere could be responsible as the vorticity would tend to be greater over the lakes with larger surface area.

[8] *Serruya et al.* [1984] applied the steady state circulation model to Lake Kinneret and Lake Constance to examine the effect of wind stress curl on circulation in these basins. Their results showed that realistic values of wind stress curl were sometimes sufficient to generate a single gyre circulation pattern in these basins, and the results were qualitatively similar to observed circulation patterns.

[9] *Strub and Powell* [1986] attribute the observed summer circulation pattern of two counter-rotating gyres in Lake Tahoe to the effect of wind stress curl induced by local mountain topography. They used a time dependent numerical model to simulate the response of the stratified lake to spatially uniform and spatially variable wind fields. They found that spatially uniform wind could reproduce the observed circulation pattern, but only after several days of model simulation. The model results with spatially variable wind generated a stronger two-gyre pattern more quickly. Their conclusion was that because the scale of the wind variation over Lake Tahoe is comparable to the size of the basin, wind stress curl is crucial in reproducing the observed two-gyre circulation pattern in the lake.

[10] A similar study in Lake Biwa by *Endoh et al.* [1995] also showed the presence of a two counter-rotating gyre circulation pattern with a dominant anticyclonic gyre. Again, anticyclonic vorticity in the wind stress field was invoked as the mechanism for strengthening the anticyclonic circulation in the lake.

[11] In Lake Geneva, which is also surrounded by mountainous terrain that tends to steer local winds, *Lemmin and D’Adamo* [1996] observed persistent cyclonic circulation in the central part of the lake. They attributed this feature to cyclonic vorticity in the diurnal wind pattern, in accordance with the direct circulation mechanism proposed by *Strub and Powell* [1986].

[12] Wind stress vorticity was also shown to be important in determining the circulation in very small Lake Belau (surface area  $\sim 1 \text{ km}^2$ ) by *Podsetchine and Schernewski* [1999]. In this case, local topography and sheltering from surrounding forests created persistent patterns of horizontal wind shear resulting in a single gyre circulation pattern.

[13] *Simons* [1986] showed that over longer periods (seasonal to multiannual) the nonlinear interactions of topographic waves in an unstratified lake can also lead to a single cyclonic gyre circulation pattern. The nonlinear response becomes important over longer periods of time when the mean wind stress (and the linear response of the circulation pattern) may become vanishingly small.

[14] There have been several theories about the ubiquity of cyclonic circulation in large and medium sized stratified lakes, including the effect of cyclonic wind vorticity caused by the asymmetry of the surface water temperature field in a stratified lake exposed to a uniform wind [*Emery and Csanady*, 1973], Lagrangian drift associated with internal Kelvin waves in a stratified lake [*Wunsch*, 1973], asymmetrical vertical mixing between upwelling and downwelling regions in a stratified lake [*Bennett*, 1975], and geostrophic circulation around a ‘domed’ thermocline [*Schwab et al.*, 1995]. These theories all depend on baroclinic effects and all result in enhanced cyclonic circulation during the stratified period.

[15] The motivation for the present paper stems from the recent comprehensive analysis of Lake Michigan’s circulation over two multiseason periods by *Beletsky and Schwab* [2001]. This paper represents the first long-term simulations of the three-dimensional circulation and thermal structure and comparison with field observations in the Great Lakes. It also provides an opportunity to examine the relative effects of wind stress curl, topography, and stratification on large-scale circulation over a period long enough to encompass the full range of atmospheric and thermal conditions that can occur in the lake. The purpose of this paper is to diagnose the relative importance of various mechanisms responsible for the large-scale circulation patterns by analyzing the vorticity balance in the lake on a monthly timescale. Five different model scenarios are used to isolate the predominant mechanisms: 1) baroclinic lake, spatially variable wind stress; 2) barotropic lake, spatially variable wind stress; 3) baroclinic lake, spatially uniform wind stress; 4) barotropic lake, spatially uniform wind stress; and 5) barotropic lake, linearized equations, spatially uniform wind stress. By comparing the results of these five model scenarios, we will show that the cyclonic wind stress curl in the winter and the effect of baroclinicity in the

**Table 1.** Hydrodynamic Model Scenarios

	Wind Stress Forcing	Stratification	Nonlinear Terms
Case A	spatially variable	Yes	Yes
Case B	spatially variable	No	Yes
Case C	spatially uniform	Yes	Yes
Case D	spatially uniform	No	Yes
Case E	spatially uniform	No	No

summer are primarily responsible for the predominantly cyclonic flow in the lake. Topographic effects are also important, but not as significant as wind stress curl and baroclinic effects. Nonlinear effects are much smaller.

## 2. Model Cases

[16] The model data used in this study are derived from the hydrodynamic model of Lake Michigan developed by *Beletsky and Schwab* [2001]. They used the Princeton Ocean Model [*Blumberg and Mellor*, 1987] to simulate the three-dimensional circulation and thermal structure in Lake Michigan for two 18 month periods in 1982–1983 and 1994–1995 on a 5 km computational grid with 20 vertical levels. Surface forcing for the hydrodynamic model consists of heat and momentum fluxes which are calculated by a bulk aerodynamic submodel based on observations of wind, dew point, air temperature, and cloud cover from an extensive network of meteorological stations around the lake. The bulk aerodynamic transfer coefficients for heat and momentum depend on wind speed and atmospheric stability. The model results from *Beletsky and Schwab* [2001], consisting of hourly gridded fields of currents and temperatures, correspond to case A in the present paper. In order to isolate particular aspects of the hydrodynamics, we made four more model runs for the same 1982–1983 and 1994–1995 periods, each with specific restrictions on the forcing functions and model physics. The five cases are outlined in Table 1. Case B uses the same wind forcing as case A, but eliminates surface heat flux so that baroclinic effects are removed. Case C includes heat flux, but substitutes hourly, spatially averaged wind stress fields for the spatially variable wind fields in the momentum flux calculation. Case D also uses spatially averaged wind stress and, in addition, eliminates baroclinicity. Case E is the same as case D, except for the elimination of nonlinear advection terms and the use of a linearized formula for bottom friction in the hydrodynamic model.

[17] *Beletsky and Schwab* [2001] showed that the full model (case A) was able to reproduce the observed large-scale circulation patterns in Lake Michigan. The seasonal (summer: May–October, winter: November–April) average currents from the 1982–1983 and 1994–1995 simulation periods are shown in Figure 1. The depth-averaged circulation was generally stronger in winter than in summer, and also more organized and cyclonic. The strongest currents and maximum cyclonic vorticity were observed and modeled when the lake was either weakly stratified or homogeneous, from November until April. The model was also able to reproduce all of the basic features of the thermal structure in Lake Michigan, including the spring thermal bar, full stratification, deepening of the thermocline during fall cooling, and finally full vertical mixing in late fall. Because of

the favorable comparison between observed currents and model results for the full model in case A, we feel that the restricted models (cases B–E) will be useful to isolate the predominant dynamic forces which affect large-scale circulation on a monthly timescale.

## 3. Vorticity Balance

[18] Following *Ezer and Mellor* [1994], the horizontal momentum equations for the vertically integrated transport as implemented in the Princeton Ocean model can be written as

$$\frac{\partial U}{\partial t} + A_x - fV = -\frac{D}{\rho_0} \frac{\partial P_b}{\partial x} - \frac{1}{\rho_0} \frac{\partial \Phi}{\partial x} + \frac{\tau_{sx}}{\rho_0} - \frac{\tau_{bx}}{\rho_0} \quad (1)$$

$$\frac{\partial V}{\partial t} + A_y + fU = -\frac{D}{\rho_0} \frac{\partial P_b}{\partial y} - \frac{1}{\rho_0} \frac{\partial \Phi}{\partial y} + \frac{\tau_{sy}}{\rho_0} - \frac{\tau_{by}}{\rho_0} \quad (2)$$

where  $U$  and  $V$  are the components of vertically integrated transport,  $A_x$  and  $A_y$  are the  $x$  and  $y$  components of the combined advection and diffusion terms,  $f$  is the Coriolis parameter,  $D$  is total water depth,

$$P_b = \rho_0 g \eta + \int_{-H}^{\eta} \rho g dz \quad (3)$$

is bottom pressure,  $\rho$  is density,  $\rho_0$  is the reference density,  $g$  is gravity,  $\eta$  is free surface displacement,  $H = D - \eta$  is the still water depth,

$$\Phi = \int_{-H}^{\eta} \rho g z dz \quad (4)$$

is potential energy,  $\tau_{sx}$  and  $\tau_{sy}$  are surface stress components, and  $\tau_{bx}$  and  $\tau_{by}$  are bottom stress components.

[19] To form the transport vorticity equation, cross-differentiate equations (1) and (2) and subtract to obtain

$$\frac{\partial \xi}{\partial t} = -\text{curl } A - \text{div}(fV) + \frac{1}{\rho_0} J(P_b, D) + \text{curl} \frac{\tau_s}{\rho_0} - \text{curl} \frac{\tau_b}{\rho_0} \quad (5)$$

(T<sub>1</sub>)      (T<sub>2</sub>)      (T<sub>3</sub>)      (T<sub>4</sub>)      (T<sub>5</sub>)      (T<sub>6</sub>)

where  $\xi = \text{curl } V$  is the transport vorticity, and  $J(a, b) = \frac{\partial a}{\partial x} \frac{\partial b}{\partial y} - \frac{\partial a}{\partial y} \frac{\partial b}{\partial x}$  is the Jacobian operator. The terms in equation (5) are identified as

- T<sub>1</sub> vorticity tendency;
- T<sub>2</sub> advection and diffusion;
- T<sub>3</sub> Coriolis term (flow divergence for constant  $f$  plane);
- T<sub>4</sub> internal pressure gradient;
- T<sub>5</sub> wind stress;
- T<sub>6</sub> bottom stress.

[20] As pointed out by *Strub and Powell* [1986], the internal pressure gradient term  $T_4$  and the curl of the wind stress  $T_5$  are the principal sources for cyclonic or anti-cyclonic vorticity in the flow. Advection and diffusion ( $T_2$ ), divergence ( $T_3$ ), and bottom stress ( $T_6$ ) are generally considered ‘sinks’. Some special cases of the transport vorticity equation are for barotropic flow where the internal



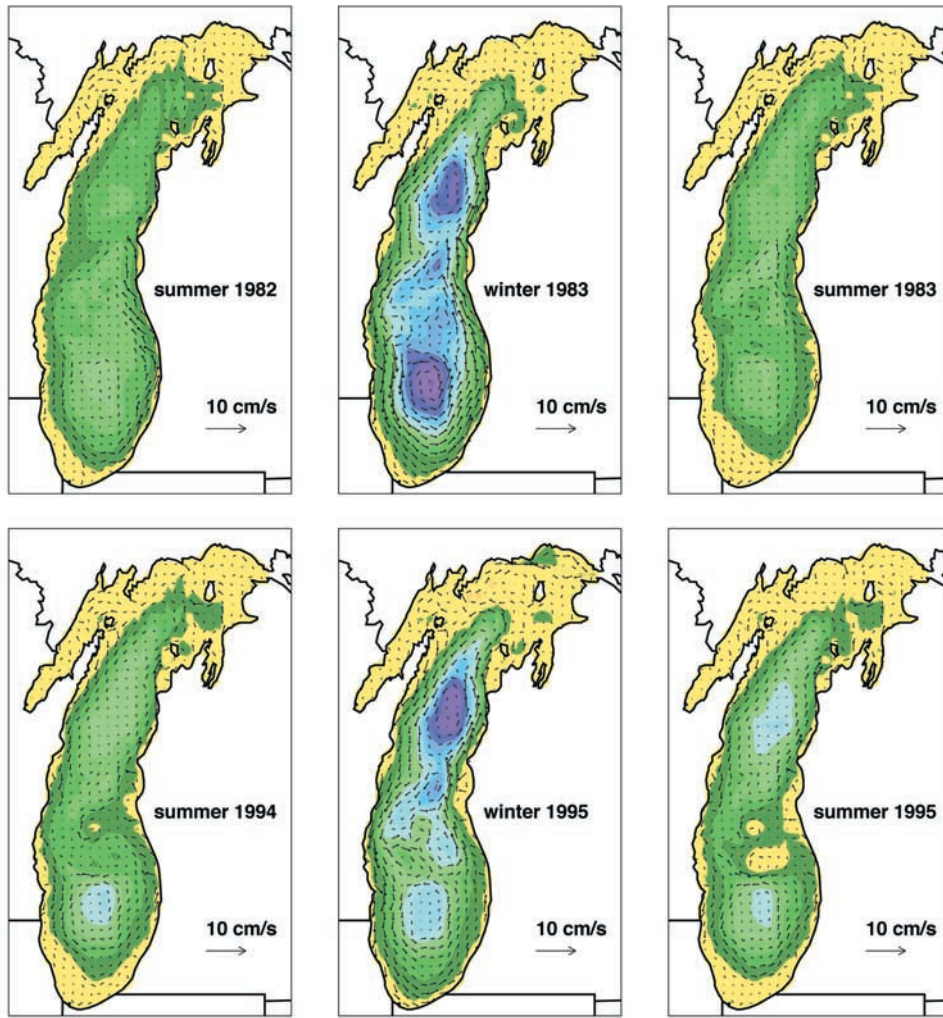


**Figure 1.** Seasonally averaged Lake Michigan currents from 1982 to 1983 and 1994 to 1995 numerical model simulations by *Beletsky and Schwab* [2001]. Summer is May–October, and winter is November–April. Colored shading represents stream function values. Yellow is positive (generally anticyclonic vorticity), and the green-blue-purple areas are negative stream function (generally cyclonic vorticity).

pressure gradients are zero and  $T_4$  vanishes, and for steady barotropic flow where  $T_1 = 0$ ,  $T_4 = 0$ , and the flow divergence ( $T_3$ ) is zero because the steady state flow is nondivergent. In steady state barotropic flow, if the advection and diffusion terms are small there is a balance between the curl of surface stress and bottom stress. In the case of linear bottom friction of the form  $\tau_b/\rho_0 = c_d V$ , this implies

$$\xi = \frac{1}{c_d} \text{curl} \frac{\tau_s}{\rho_0} \quad (6)$$

or transport vorticity is simply proportional to the curl of the wind stress.

[21] If equations (1) and (2) are divided by depth before cross differentiation, one obtains the current vorticity equation

$$\frac{\partial \zeta}{\partial t} = \underbrace{-\text{curl} \left( \frac{A}{D} \right)}_{(T_1)} - \underbrace{\text{div}(f\mathbf{v})}_{(T_2)} - \underbrace{\frac{1}{\rho_0} \text{curl} \left( \frac{1}{D} \nabla \Phi \right)}_{(T_3)} + \underbrace{\text{curl} \left( \frac{\tau_s}{\rho_0 D} \right)}_{(T_4)} - \underbrace{\text{curl} \left( \frac{\tau_b}{\rho_0 D} \right)}_{(T_5)} \quad (7)$$

where  $\zeta = \text{curl} \mathbf{v}$  is the current vorticity. Note that in the current vorticity equation, the internal pressure gradient term no longer involves surface elevation, but wind stress and bottom stress are now divided by depth. As *Simons* [1980] points out, the mean flow vorticity usually gives a more meaningful indication of the horizontal current pattern than the transport vorticity in shallow basins and will be used here specifically to demonstrate the effect of topography on lakewide average circulation.

## 4. Results

### 4.1. Total Vorticity Balance

[22] For each model run (cases A–E), the six terms in equations (5) and (7) are evaluated at each grid square and then averaged over the model domain. Monthly averages of the hourly values for the five cases for both the 1982–1983 and 1994–1995 periods are plotted in Figures 2 and 3. The average transport vorticity  $\xi$  (divided by  $10^5$  s to convert to units comparable to the rest of the terms in Equation 5) is also plotted in Figure 2, as is the current vorticity  $\zeta$  (also

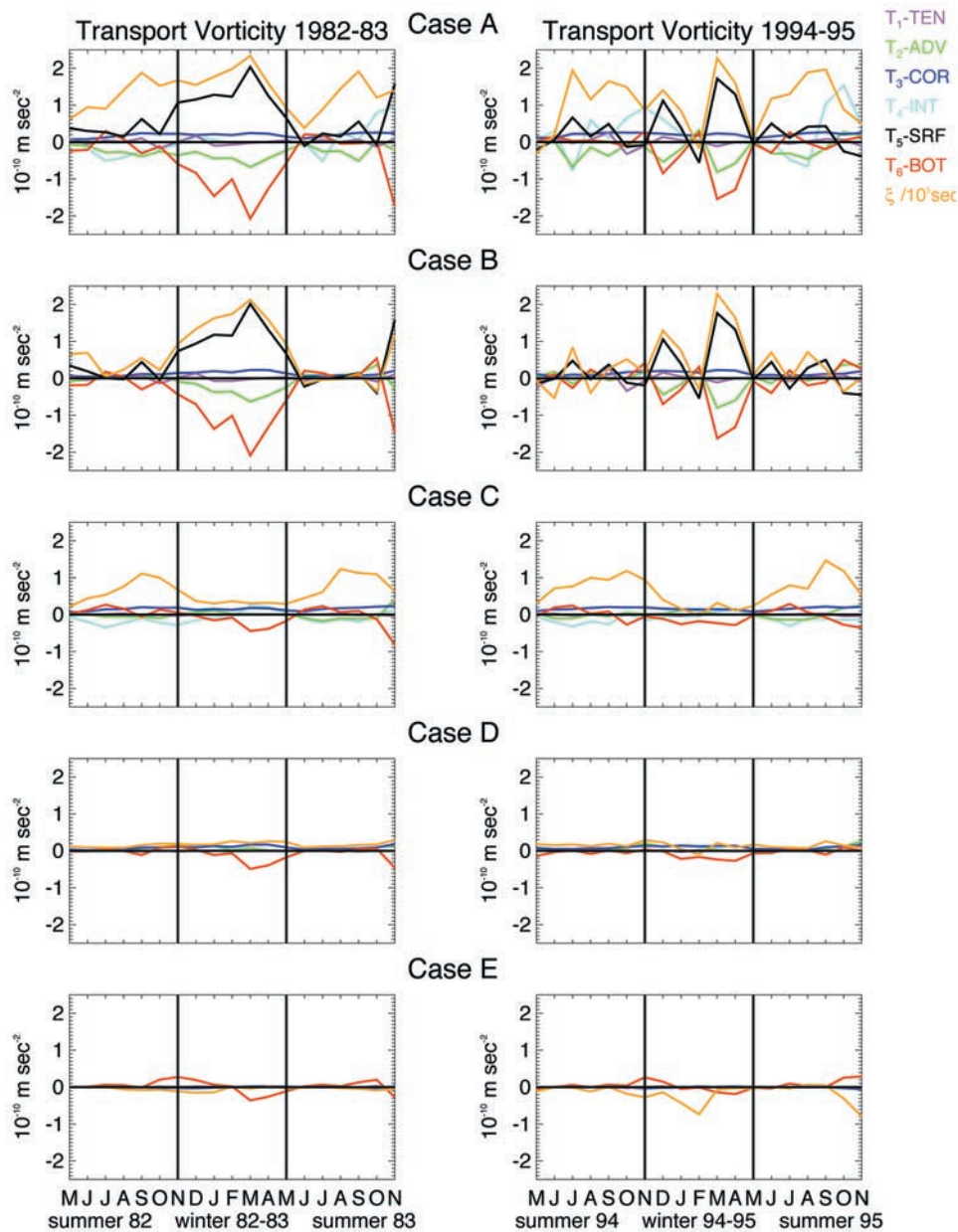


**Figure 2.** Monthly average transport vorticity balance for 1982–1983 and 1994–1995 model simulations. Case A: Spatially variable wind, baroclinic; case B: spatially variable wind, barotropic; case C: spatially uniform wind, baroclinic; case D: spatially uniform wind, barotropic; and case E: spatially uniform wind, barotropic, linear.

divided by  $10^5$  s) in Figure 3. The results of *Beletsky and Schwab* [2001] for the full model equations (case A) show the dominance of net cyclonic vorticity (positive values) during both modeling periods. During the summer stratified periods, all the individual terms in the transport vorticity balance have comparable magnitudes. During the winter, wind stress and bottom stress dominate the balance. There is a tendency for total vorticity to follow wind stress vorticity, especially during the winter months. In case B (barotropic, spatially variable wind), the total transport vorticity and total current vorticity are considerably reduced in the summer months and tend to follow wind stress vorticity throughout the year. In case C (baroclinic, spatially uniform

wind stress) there is strong cyclonic vorticity in the summer. Case D (barotropic, spatially uniform wind stress) and case E (linear) show much smaller values for all terms in the transport vorticity balance. In the current vorticity plot for cases D and E, there is a similar balance between surface stress and bottom stress as case C, but total vorticity is much smaller in the summer periods than in case C.

#### 4.2. Effect of Wind Stress Curl

[23] In order to isolate the effect of wind stress curl on the vorticity balance, Figure 4 shows the monthly average wind stress vorticity term from case A and the difference in transport vorticity  $\xi$  between cases A and C and cases B

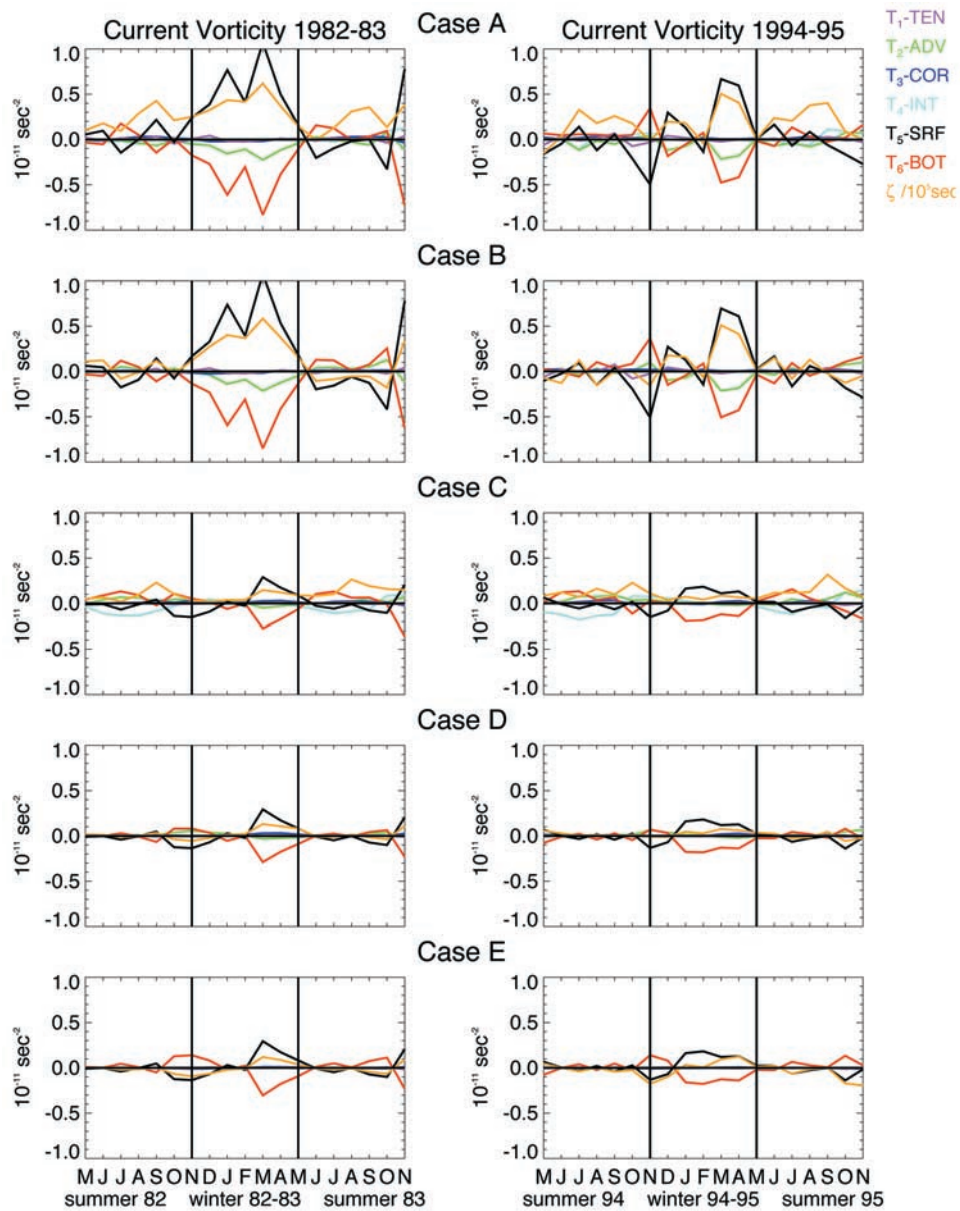


**Figure 3.** Monthly average current vorticity balance for 1982–1983 and 1994–1995 model simulations. Cases are as in Figure 2.

and D. Since the only difference between baroclinic cases A and C (and barotropic cases B and D) is that spatially uniform wind stress is used instead of spatially variable wind stress, we attribute the difference in transport stream function between the cases solely to wind stress curl. Figure 4 supports this conclusion in that the transport vorticity differences between the barotropic cases B and D and the baroclinic cases A and C are nearly identical, indicating that any effect of baroclinicity has been removed. There is also strong correlation between the transport vorticity curves and the wind stress vorticity term in the top panel. Current vorticity curves show a similar correlation.

#### 4.3. Effect of Baroclinicity

[24] To isolate the effect of baroclinicity on the vorticity balance, Figure 5 shows the difference in transport vorticity

between cases A and B with spatially variable wind stress and cases C and D with spatially uniform wind stress. Since the only difference between cases A and B (and C and D) is baroclinicity, we attribute the difference in transport stream function to baroclinic effects. The upper two sets of panels (cases A–B and cases C–D) show a net increase of cyclonic vorticity due to baroclinicity during the summer stratified months of both simulation periods. The middle set of panels (cases C–D) represent the vorticity generated purely by internal buoyancy effects. The third set of panels in Figure 5 shows the difference in vorticity between case A and the combination of cases B and C. Since case B includes spatially variable wind stress, but uniform surface water temperature, and case C includes baroclinic effects, but uses spatially uniform wind stress, the third set of panels isolates the *Emery and Csanady* [1973] mechanism for



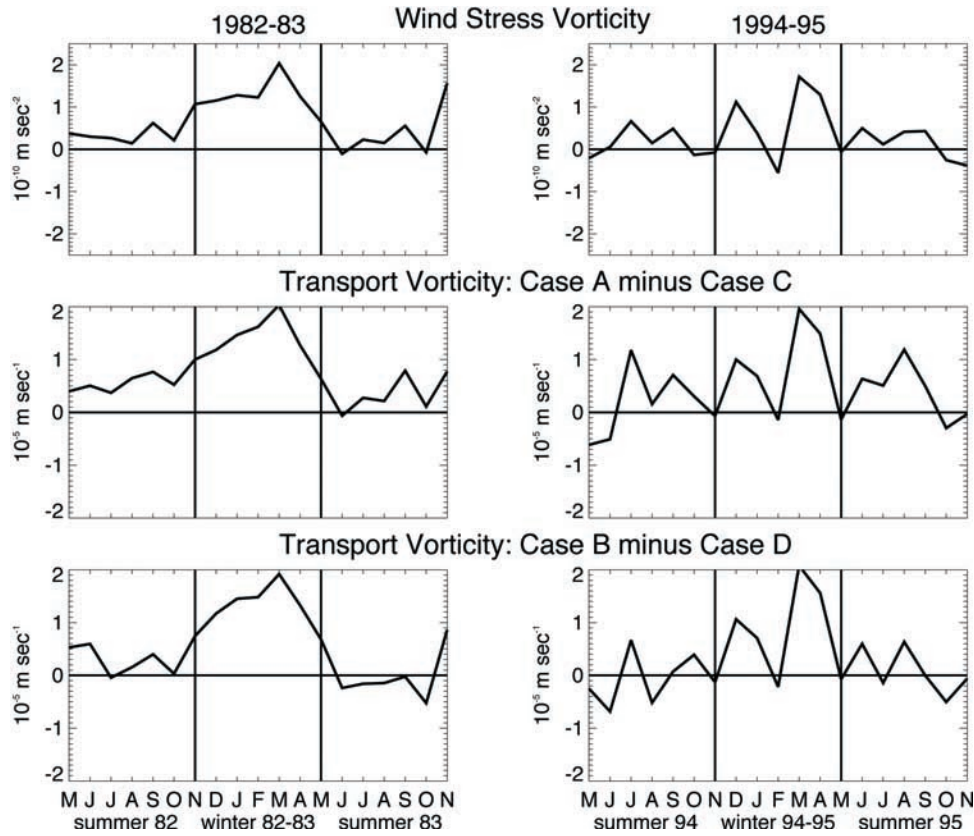


**Figure 4.** (top) Monthly average wind stress vorticity from case A, (middle) difference in transport vorticity between case A and case C, and (bottom) difference in transport vorticity between case B and case D.

generation of cyclonic vorticity. In their mechanism, cyclonic wind stress vorticity results from horizontal gradients in surface water temperature generated by upwelling on the left side of the wind. The Emery-Csanady effect is smaller, but still significant.

#### 4.4. Effect of Nonlinearity

[25] Figure 6 shows the monthly mean values of the advection/diffusion term (T2 in equation 5) from case D (uniform wind stress, barotropic) as well as the difference in transport vorticity between case D and the linearized case E. The difference in total transport vorticity appears to be related to the advection/diffusion term as suggested by *Simons* [1986]. The effect on vorticity is stronger in the 1994–1995 simulation than in the 1982–1983 simulation. The advection/diffusion term is also largest in the fall of both periods.

#### 4.5. Effect of Topography

[26] In order to examine the effect of topography on the vorticity balance in Lake Michigan, we consider the steady state form of the current vorticity equation (7) in the absence of rotation with linear bottom friction,  $\tau_b/\rho_0 = c_d D \mathbf{v}$ . The reason we use the current vorticity equation in this case is that the effect of topography is more apparent than for the transport vorticity equation. Equation (6) shows that the steady state transport vorticity with linear bottom friction depends only on the curl of the wind stress. For spatially uniform wind stress, the transport vorticity is zero.

For the linear bottom friction case, the current vorticity balance (equation (7)) reduces to

$$\zeta = \frac{1}{c_d} \text{curl} \frac{\tau_s}{\rho_0 D} = -\frac{\tau_s}{c_d \rho_0} \times \nabla \frac{1}{D} + \frac{1}{c_d \rho_0 D} \text{curl} \tau_s \quad (8)$$

Equation (8) shows that the current vorticity for this case depends on topography (first term on right-hand side) as well as wind stress curl (second term on right-hand side). Specifically, for spatially uniform wind stress the second term vanishes and equation (8) can be written

$$\zeta = -\frac{\tau_s}{c_d \rho_0} \times \nabla \frac{1}{D} = \frac{\tau_s \times \nabla D}{c_d \rho_0 D^2} \quad (9)$$

So for a uniform wind, vorticity is generated where the wind stress vector crosses isobaths. For symmetric geometries, like a circular paraboloid, the basin-averaged vorticity will be zero. For arbitrary geometries, the exact shape of the basin will determine the net amount of vorticity generated for a specific wind direction. Less net vorticity will be generated in relatively flat basins. More net vorticity will be generated in basins with asymmetric bathymetry.

[27] For the Lake Michigan case, we calculated the steady state response of the linearized barotropic model (case E) for uniform westerly and uniform southerly wind. In this case, the steady state response to arbitrary wind direction is

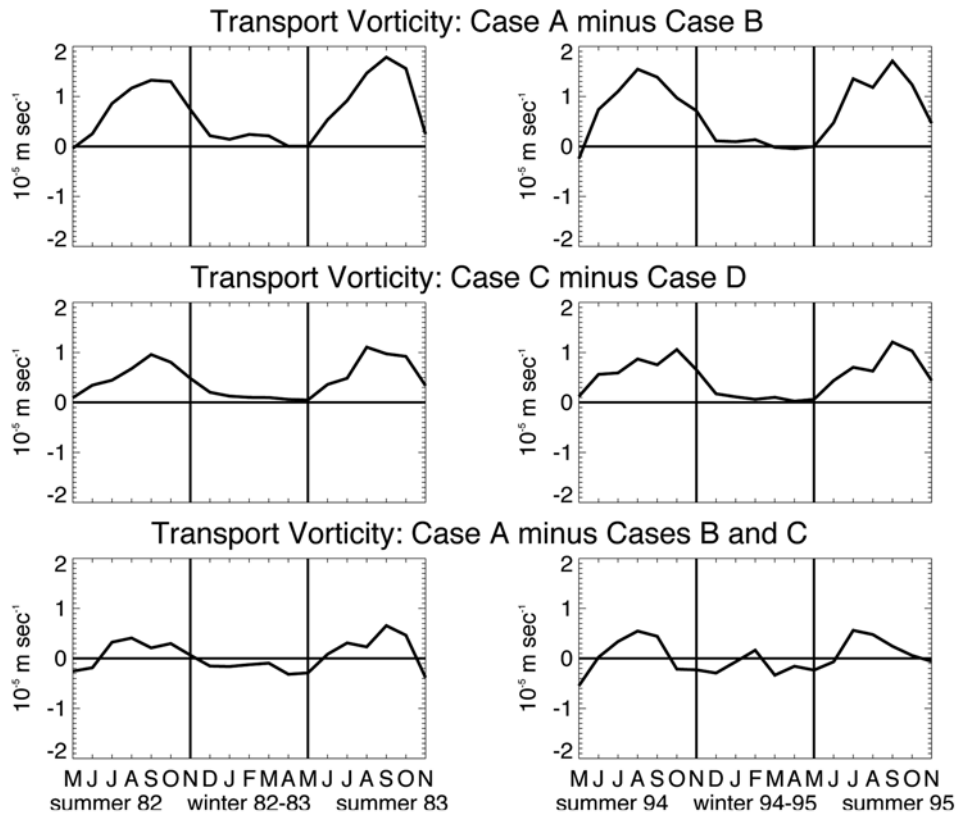


**Figure 5.** (top) Difference in transport vorticity between case A and case B, (middle) difference in transport vorticity between case C and case D, and (bottom) difference in transport vorticity between case A and cases B and C.

the sum of the responses for the individual components of the wind stress vector, i.e.,

$$\zeta = a\tau_s^x + b\tau_s^y \quad (10)$$

For Lake Michigan we found  $a = -2.2 \times 10^{-7} \text{ cm}^2 \text{ dyn}^{-1} \text{ s}^{-1}$  and  $b = -3.2 \times 10^{-7} \text{ cm}^2 \text{ dyn}^{-1} \text{ s}^{-1}$ . This implies that the maximum cyclonic vorticity is generated for a wind

from between NE and NNE and the maximum anticyclonic vorticity for a wind from between SSW and SW. The mean wind stress components for each month of the 1982–1983 and 1994–1995 simulation periods are shown in the top panel of Figure 7 (eastward component by a solid line, northward component by a dotted line). The middle panel shows the steady state current vorticity calculated from

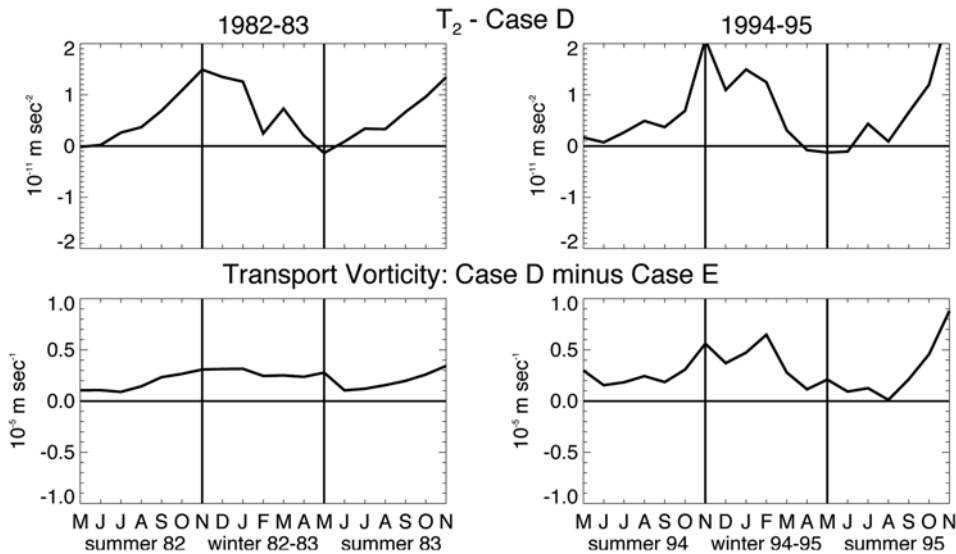


**Figure 6.** (top) Advection/diffusion term  $T_2$  from case D and (bottom) difference in transport vorticity between case D and case E.



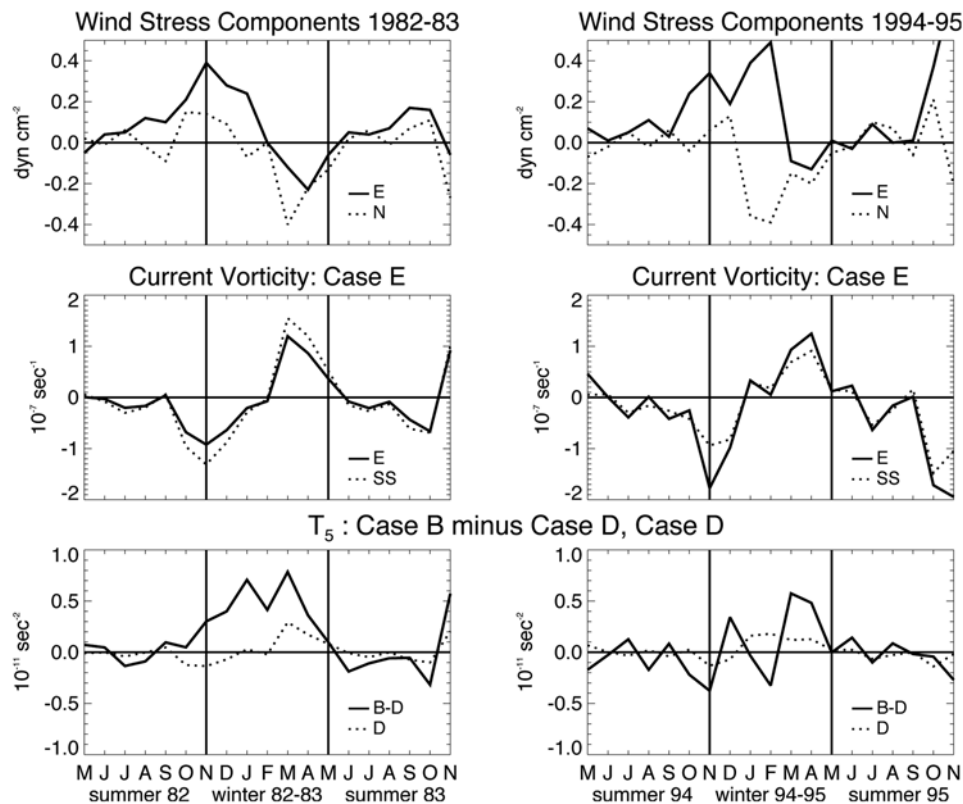


**Figure 7.** (top) Monthly mean wind stress components for 1982–1983 and 1994–1995 (solid line is eastward component, and dotted line is northward component), (middle) current vorticity from case E and steady state calculations, and (bottom) difference in current vorticity between case B and case D (solid line), as well as current vorticity from case D (dotted line).

equation (10) (dotted line) and the monthly mean current vorticity from case E (solid line). The largest topographically induced anticyclonic vorticity occurs in the fall when mean winds are from the W to SW and the largest cyclonic vorticity occurs in the spring when mean winds are from the NE. The case E current vorticity is very similar to the steady state vorticity, indicating that the linearized barotropic response of the lake circulation to spatially uniform wind provides a good indication of the topographic contribution to the vorticity balance in the lake. The lower panel shows the difference in the wind stress curl term ( $T_5$ ) from the current vorticity balance (equation (7)) between case B and case D (solid line), as well as the  $T_5$  term itself from case D (dotted line). The difference between case B and case D is equivalent to the second term on the right-hand side of equation (8) and  $T_5$  from case D is equivalent to the first term. The wind stress curl effect (solid line) is almost always 2–3 times larger than the topographic effect (dotted line). The wind stress curl term in the absence of baroclinic effects is mostly cyclonic in the winter periods, and small or slightly anticyclonic in the summer.

## 5. Discussion and Conclusions

[28] By analyzing the Lake Michigan hydrodynamic model results from 1982–1983 and 1994–1995 under barotropic and baroclinic conditions and also for spatially variable and spatially uniform wind stress conditions, we

have shown that direct forcing from the wind stress curl is the dominant mechanism determining the vorticity of the mean circulation pattern in the lake during the unstratified winter season. Nonlinear effects contribute to the net cyclonic circulation, but their impact is much smaller than the direct influence of cyclonic wind stress curl. The predominantly cyclonic wind stress curl during the winter period is the result of the large heat capacity of the lakes which tends to generate a mesoscale low pressure system over the lakes during periods when air temperatures are below water temperatures [Petterssen and Calabrese, 1959; Weiss and Sousounis, 1999]. The magnitude of the cyclonic wind stress curl is almost always 2–3 times larger than the topographic effect.

[29] During the stratified period, the lake circulation was also found to be predominantly cyclonic. We showed that the summertime cyclonic vorticity is due mainly baroclinic effects, although a significant amount of cyclonic vorticity results from gradients in atmospheric stability over the lake, as proposed by Emery and Csanady [1973].

[30] Vorticity can also be generated from a uniform wind in the stratified or unstratified period simply from the asymmetric topography of the lake. In Lake Michigan, this effect is usually considerably smaller than the direct effect of wind stress curl.

[31] The nonlinear rectification of topographic waves proposed by Simons [1986] as a mechanism for generating cyclonic vorticity over longer periods does not appear to be significant on a monthly timescale.

[32] These results are consistent with monthly circulation patterns observed in Lake Ontario during IFYGL by *Pickett and Richards* [1975] and *Pickett* [1976, 1977]. In the summer, baroclinicity appears to be responsible for net cyclonic circulation. In the winter, cyclonic wind stress curl can often overwhelm the two-gyre wind-induced circulation pattern even though *Pickett* [1977] did not think that observed mean horizontal wind shears were sufficient. The monthly average wind vorticities for Lake Michigan from the 1982–1983 and 1994–1995 simulation periods were on the order of  $5 \times 10^{-6} \text{ s}^{-1}$ , which is over an order of magnitude larger than the  $10^{-7} \text{ s}^{-1}$  used by *Pickett* [1977], but more consistent with the IFYGL 6-month averages estimated by *Chen* [1977].

[33] The long term (6 month) mean cyclonic circulation patterns for the larger Great Lakes (Superior, Michigan and Huron) as described by *Beletsky et al.* [1999] are consistent with a dominant wind stress curl effect. The two gyre pattern in the smaller lakes (Ontario and Erie) during the winter may indicate that the smaller surface area reduces the importance of synoptic-scale wind vorticity. During the summer, the large lakes exhibited more complex, but predominantly cyclonic circulation. Lake Ontario was also cyclonic, but Lake Erie (the shallowest lake, and warmest during the summer) was mostly anticyclonic, which may be a result of anticyclonic wind stress vorticity induced by mesoscale high pressure in the atmosphere over the lake.

[34] The circulation patterns in Lake Kinneret, Lake Constance, Lake Geneva, and Lake Belau [*Serruya et al.*, 1984; *Lemmin and D'Adamo*, 1996; *Podsetchine and Schernewski*, 1999] are all consistent with the dominance of cyclonic wind stress curl for these basins as well. In Lake Tahoe and Lake Biwa the wind stress curl is predominantly anticyclonic and the mean circulation in both lakes is consistent with direct wind forcing [*Strub and Powell*, 1986; *Endoh et al.*, 1995]. Each of these lakes has a different combination of topographic and baroclinic effects in the vorticity balance, but even in lakes as small as Biwa and Kinneret, and even tiny Lake Belau, the effect of wind stress curl is predominant. It should be noted however that the wind stress curl for these smaller lakes is usually produced from orographic effects, whereas in Lake Michigan (and the other large Great Lakes), the wind stress vorticity appears to be a result of the lake surface on mesoscale atmospheric circulation.

[35] In summary, we found here that by analyzing the vorticity balance for five numerical model simulations of Lake Michigan circulation with various wind stress and stratification scenarios, the effect of mean cyclonic wind stress over the lake during winter months was usually much stronger than topographic effects and resulted in a predominantly cyclonic circulation pattern. During the summer stratified season, net cyclonic vorticity was due mainly to baroclinic effects, with an indication that cyclonic wind stress vorticity generated by atmospheric stability gradients could also be a significant factor. Over monthly timescales, nonlinear effects such as the rectification of barotropic topographic waves did not appear to contribute significantly to net cyclonic vorticity.

Research Laboratory and University of Michigan provided funding for this research. This is NOAA/GLERL contribution 1232.

## References

- Beletsky, D., and D. J. Schwab, Modeling circulation and thermal structure in Lake Michigan: Annual cycle and interannual variability, *J. Geophys. Res.*, **106**, 19,745–19,771, 2001.
- Beletsky, D., J. H. Saylor, and D. J. Schwab, Mean circulation in the Great Lakes, *J. Great Lakes Res.*, **25**, 78–93, 1999.
- Bennett, J. R., Another explanation of the observed cyclonic circulation of large lakes, *Limnol. Oceanogr.*, **20**, 108–110, 1975.
- Birchfield, G. E., Horizontal transport in a rotating basin of parabolic depth profile, *J. Geophys. Res.*, **72**, 6155–6163, 1967.
- Blumberg, A. F., and G. L. Mellor, A description of a three-dimensional coastal ocean circulation model, in *Three-Dimensional Coastal Ocean Models*, *Coastal Estuarine Sci.*, vol. 4, edited by N. S. Heaps, pp. 1–16, AGU, Washington, D. C., 1987.
- Chen, W. Y., Analysis of vorticity and divergence fields and other meteorological parameters over Lake Ontario during IFYGL, *Mon. Weather Rev.*, **105**, 1298–1309, 1977.
- Csanady, G. T., The arrested topographic wave, *J. Phys. Oceanogr.*, **8**, 47–62, 1978.
- Emery, K. O., and G. T. Csanady, Surface circulation of lakes and nearly land-locked seas, *Proc. Natl. Acad. Sci. USA*, **70**, 93–97, 1973.
- Endoh, S., M. Watanabe, H. Nagata, F. Maruo, T. Kawae, C. Iguchi, and Y. Okumura, Wind fields over Lake Biwa and their effect on water circulation, *Jpn. J. Limnol.*, **4**, 269–278, 1995.
- Ezer, T., and G. L. Mellor, Diagnostic and prognostic calculations of the North Atlantic circulation and sea level using a sigma coordinate ocean model, *J. Geophys. Res.*, **99**, 14,159–14,171, 1994.
- Lemmin, U., and N. D'Adamo, Summertime winds and direct cyclonic circulation: observations from Lake Geneva, *Ann. Geophys.*, **14**, 1207–1220, 1996.
- Murty, T. S., and D. B. Rao, Wind-generated circulations in lakes Erie, Huron, Michigan, and Superior, in paper presented at 13th Conference on Great Lakes Research, Int. Assoc. of Great Lakes Res., State Univ. College, Buffalo, N. Y., 1970.
- Pettersen, S., and P. A. Calabrese, On some weather influences due to warming of the air by the Great Lakes in winter, *J. Meteorol.*, **16**, 646–652, 1959.
- Pickett, R. L., Lake Ontario circulation in November, *Limnol. Oceanogr.*, **21**, 608–611, 1976.
- Pickett, R. L., The observed winter circulation of Lake Ontario, *J. Phys. Oceanogr.*, **7**, 152–156, 1977.
- Pickett, R. L., and F. P. Richards, Lake Ontario mean temperatures and currents in July, 1972, *J. Phys. Oceanogr.*, **5**, 775–781, 1975.
- Podsetchine, V., and G. Schernewski, The influence of spatial wind homogeneity on flow patterns in a small lake, *Water Res.*, **33**, 3348–3356, 1999.
- Rao, D. B., and T. S. Murty, Calculation of the steady-state wind-driven circulations in Lake Ontario, *Arch. Meteorol. Geophys. Bioklimatol., Ser. A*, **19**, 195–210, 1970.
- Saylor, J. H., J. C. K. Huang, and R. O. Reid, Vortex modes in southern Lake Michigan, *J. Phys. Oceanogr.*, **10**, 1814–1823, 1980.
- Schwab, D. J., Numerical simulation of low-frequency current fluctuations in Lake Michigan, *J. Phys. Oceanogr.*, **13**, 2213–2224, 1983.
- Schwab, D. J., W. P. O'Connor, and G. L. Mellor, On the net cyclonic circulation in large stratified lakes, *J. Phys. Oceanogr.*, **25**, 1516–1520, 1995.
- Serruya, S., E. Hollan, and B. Bitsch, Steady winter circulations in Lakes Constance and Kinneret driven by wind and main tributaries, *Arch. Hydrobiol.*, **70**, 33–110, 1984.
- Simons, T. J., Circulation models of lakes and inland seas, *Can. Bull. Fish. Aquat. Sci.*, **203**, 146 pp., 1980.
- Simons, T. J., The mean circulation of unstratified water bodies driven by nonlinear topographic wave interaction, *J. Phys. Oceanogr.*, **16**, 1138–1142, 1986.
- Strub, P. T., and T. P. Powell, Wind-driven surface transport in stratified closed basins: Direct versus residual circulations, *J. Geophys. Res.*, **91**, 8497–8508, 1986.
- Weiss, C. C., and P. J. Sousounis, A climatology of collective lake disturbances, *Mon. Weather Rev.*, **127**, 565–574, 1999.
- Wunsch, C., On the mean drift in large lakes, *Limnol. Oceanogr.*, **18**, 793–795, 1973.

[36] **Acknowledgments.** The USEPA Great Lakes National Program Office, NOAA Coastal Ocean Program and the Cooperative Institute for Limnology and Ecosystems Research/NOAA Great Lakes Environmental

D. Beletsky, Department of Naval Architecture and Marine Engineering, University of Michigan, Ann Arbor, MI 48105, USA.

D. J. Schwab, NOAA Great Lakes Environmental Research Laboratory, Ann Arbor, MI 48109, USA. (David.Schwab@noaa.gov)